PERGAMON

International Journal of Heat and Mass Transfer 45 (2002) 2539–2547

International Journal of HEAT and MASS TRANSFER

www.elsevier.com/locate/ijhmt

Wickless network heat pipes for high heat flux spreading applications

Y. Cao *, M. Gao

Department of Mechanical Engineering, Florida International University, University Park, Miami, FL 33199, USA

Received 16 July 2001; received in revised form 26 October 2001

Abstract

The concept of the network heat pipe employing the boiling heat-transfer mechanism in a narrow space is described. Two flat-plate wickless network heat-pipes (or thermal spreaders) are designed, fabricated, and tested based on this concept. The fabricated thermal spreaders, which are made of copper or aluminum, are wickless, cross-grooved heat transfer devices that spread a concentrated heat source to a much larger surface area. As a result, the high heat flux generated in the concentrated heat source may be dissipated through a finned surface by air cooling. The network heat pipes are tested under different working conditions and orientations relative to the gravity vector, with water and methanol as the working fluids. The maximum heat fluxes achieved are about 40 W/cm^2 for methanol and 110 W/cm^2 for water with a total heat input of 393 W.

1. Introduction

As the size of electronic devices becomes progressively smaller, the heat flux in electronic devices becomes increasingly higher. It is anticipated that the heat flux in many power electronic devices may well exceed the 100 W/cm^2 level in the near future. Heat pipes are very effective heat transfer devices and can be used to augment the thermal conductive path in order to spread a concentrated heat source over a much larger surface area. As a result, the high heat flux at the heat source can be reduced to a much smaller and manageable level that can be dissipated through conventional cooling methods.

The heat pipe used for electronic cooling purposes is usually a wicked capillary force-driven heat pipe, with a working temperature range of about 50–120 °C. The high heat-flux levels commonly handled by this type of heat pipe are on the order of 10 W/cm^2 [1,2]. Although a higher heat-flux level may be achieved by this type of heat pipe, special wick structures in the heat pipe are usually needed, which significantly increases the manufacturing costs of the heat pipe. Akachi et al. [3] and Akachi and Polasek [4] proposed and tested a variety of wickless pulsating heat pipes. They described the pulsating heat pipes as a new type of heat pipe in which heat transfer from the evaporator to the condenser is not realized by the countercurrent liquid–vapor flows as in the conventional heat pipes, but by means of a pulsating movement of a working fluid in the axial direction of smooth capillary tubes or tunnels. Fig. 1(a) shows a typical pulsating heat pipe with a number of turns of bent tubes. Fig. 1(b) shows a typical plate pulsating heat pipe with a number of turns of tunnels fabricated in the metal plate. The primary application of the pulsating heat pipe, as described by Akachi and Polasek [4] and Maezawa et al. [5], was to transfer heat from the evaporator end to the condenser end. The advantage of the pulsating heat pipe is that the heat pipe is wickless with low manufacturing costs, yet it may work at any orientation, sometimes even against gravity. The typical heat flux in the evaporator section as reported by Akachi et al. [3] was about 0.25 W/cm^2 using R142b as the working fluid. The drawback of the pulsating heat pipe was the relatively large temperature fluctuation due to the pulsating motion of the working fluid in the heat pipe. The amplitude of the temperature fluctuation, as reported by Akachi et al. [3], was about 5–6 °C with a total heat input of 80 W (0.2 W/cm^2) in the horizontal

* Corresponding author. Tel.: +1-305-348-2205; fax: +1-305-348-1932.

E-mail address: cao@eng.fiu.edu (Y. Cao).

0017-9310/02/$ - see front matter
PII: S0017-9310(01)00338-6

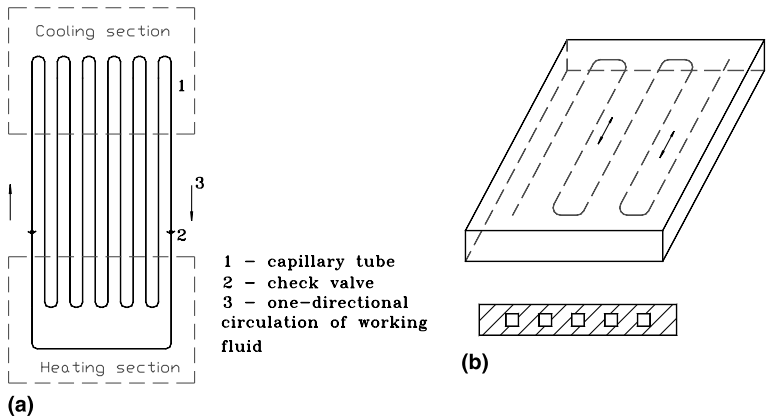

Fig. 1. Pulsating heat pipes: (a) meandering continuous tubes; (b) tunnel pulsating heat pipe.

heat-transfer mode. The fluid-charge ratio varied from 30% to 70% for the testing results presented.

Boiling heat transfer within vertical narrow gaps has been studied by several authors [6,7]. The experimental results by Chang and Yao [6] show that when the gap width is less than about 3 mm, the growth of the bubbles in the gap is restricted by the gap walls, and some bubbles coalesce with each other, resulting in the formation of a large vapor plug. In the intermittent period of vapor jets, the bulk liquid flows down along the walls into the gap. Even for a gap width of 0.2 mm, a thin liquid film apparently exists beneath the vapor plug on the vertical walls, and the boiling heat transfer coefficient rises to a higher value than that for nucleate pool boiling. Chang and Yao [6] studied the critical heat fluxes of vertical narrow annuli with closed bottoms. They considered the phenomenon as a countercurrent two-phase flow, and adopted Wallis's countercurrent flooding relation [8] to correlate their critical flux with good agreement (Fig. 2).

Katto et al. [9] studied nucleate and transition boiling in a narrow space between two horizontal, parallel disk surfaces. The space gap was created by holding an 11 mm diameter glass disc in a coaxial position above a heated 11 mm diameter horizontal, upward-facing copper disk. It was found that the state of the boiling, liquid supply to the heated surface and the occurrence of burnout were significantly affected by the gap space. They concluded that a very thin "nucleate boiling liquid layer" existed on the heated surface in the high heat-flux region. Fig. 3 shows that vapor bubbles were generated in this layer and erupted upwards, forming a vapor mass in the gap. Liquid penetrated into the gap space as the vapor mass started to detach from the periphery of the

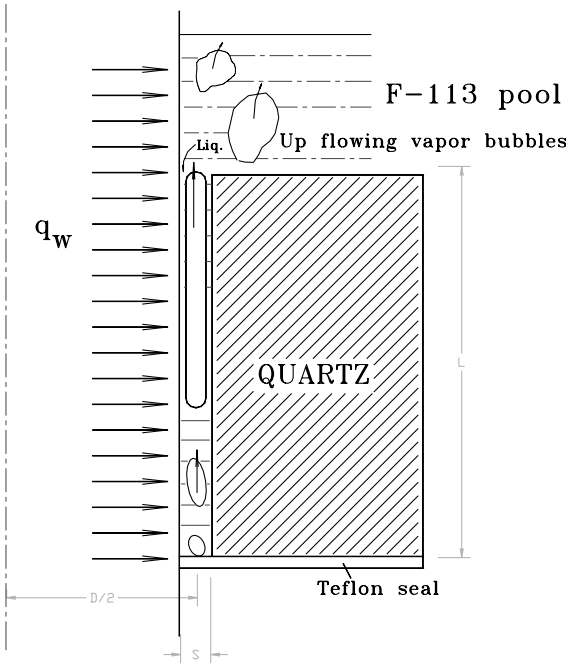

Fig. 2. The fluid behavior in narrow vertical annuli with closed bottom [6].

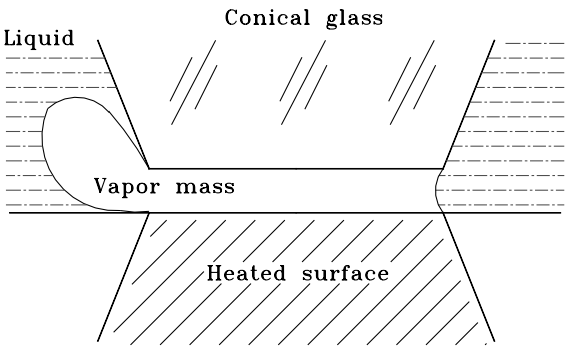

Fig. 3. Vapor and liquid interchange at the heated surface [9].

heated surface to fill the volume that was initially occupied by the vapor. The vapor and liquid interchange in the gap space is largely irregular and random through different locations around the periphery of the heated surface. The aforementioned boiling heat transfer process is related only to conventional pool boiling and is independent of the particular heat pipe devices that may be used. However, the authors believe that by employing the boiling mechanism in a narrow space, the performance of the pulsating heat pipe can be substantially improved [10].

2. Network heat pipe and its design and fabrication

The objective of this study is to develop a wickless heat pipe or thermal spreader, which can spread a large amount of heat from a concentrated heat source to a much larger surface area. For this purpose, the vapor and liquid interchange in the evaporator of the heat pipe should be adequate to reduce the temperature fluctuation at the heated surface. Because the interchange of vapor and liquid is largely random along the periphery of the heated surface, a sufficiently large number of passages should be provided for releasing generated vapor from and supplying liquid to the heated surface. Also, these passages should run throughout the entire spreader to facilitate a better communication between the different locations of the spreader. In addition, a large contact surface area between the heat source and working fluid is beneficial for the reduction of the heat flux at the boiling/evaporation surface and for the purpose of retaining a liquid sub-layer at the surface. Based on the concept discussed, two network heat pipes were fabricated and tested. As shown in Fig. 4, the first network heat pipe (HP1) consists of two aluminum T6-6061 flat-plates that are 1.60 and 3.0 mm thick, respectively. Both plates are square with about 200 mm on a side. Aluminum T6-6061 was chosen because of its better machinability and high resistance to warpage. A perpendicular network of crossed grooves was provided on one side of the 3.0 mm aluminum plate through a milling process. The milling was accomplished through the use of a computer numerically controlled (CNC) milling machine. The grooves milled are 2 mm in width and 2 mm in depth with a pitch of 4 mm. The smooth 1.6 mm aluminum plate was then welded to the machined side of the 3.0 mm aluminum plate to form the network heat pipe. The configuration and cut-off view of the network heat pipe is schematically shown in Fig. 4(a). The second flat-plate network heat pipe (HP2) is made of copper with 150 mm on a side and 7 mm in thickness. It con-

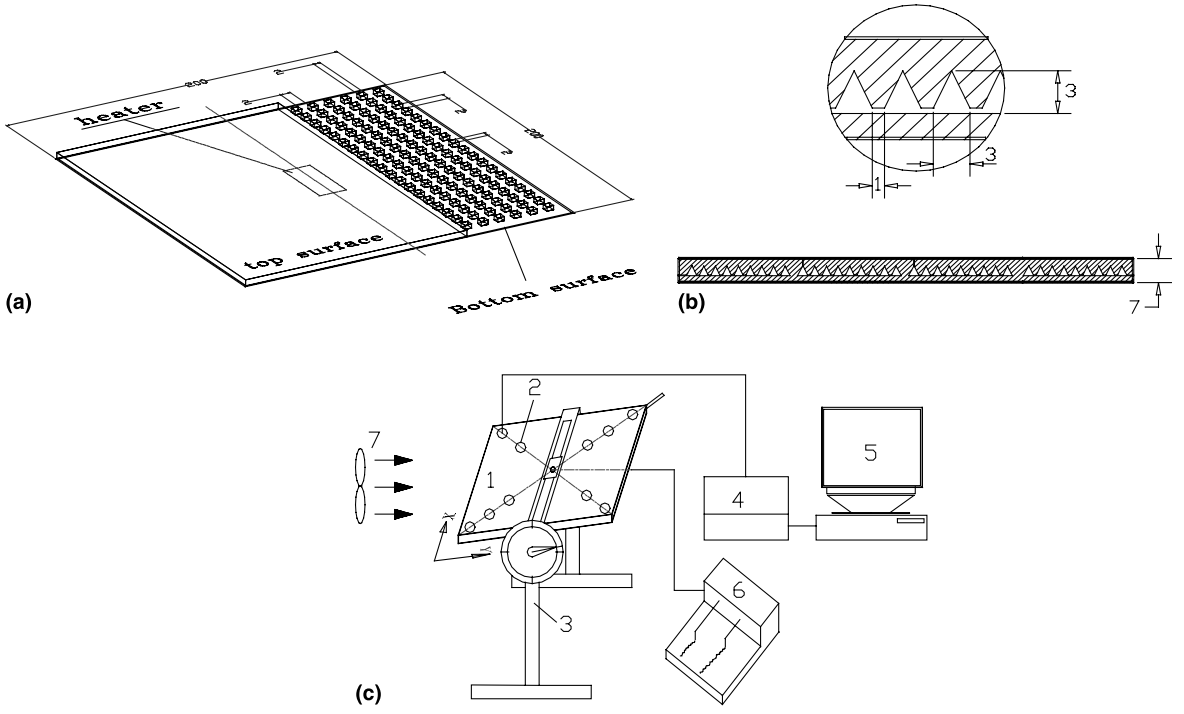

1-network heat pipe; 2-thermocouples; 3-support frame; 4-scannig thermocouple thermometer; 5-computer; 6-chart recorder; 7-cooling fan.

Fig. 4. Network heat pipe 1 (a), network heat pipe 2 (b), and experimental setup (c). (All dimensions are given in mm.)

tains crossed triangular grooves that are cut with the electric-discharge-machining (EDM) method. The schematic of the second heat pipe is shown in Fig. 4(b). After the network heat pipes were evacuated and charged with an amount of working fluid, they were ready to be tested.

The heat transfer working mechanism of the network heat pipe is similar to that of boiling heat transfer in a narrow space. When the heat flux from the heater is relatively high, vapor bubbles are generated at the heated surface, namely, the evaporator, of the network heat pipe. Because the vapor space in the heat pipe is relatively small, the bubbles are restricted by the channel walls and coalesce together, forming relatively large-sized vapor plugs. When the vapor pressure in the vapor plugs becomes sufficiently high, the vapor ejects out of the evaporator into the surrounding space, namely, the heat-pipe condenser. This results in a decrease in the vapor pressure in the evaporator region. As a result, liquid flows from the condenser into the evaporator through the periphery of the heated surface and forms liquid layers on the heated surface. Intense evaporation occurs at the liquid film surface and the vapor pressure in the evaporator begins to rise again, and the event mentioned above is being repeated. If the cycle period of the aforementioned vapor–liquid interchange process at the evaporator is very short, the vapor can be considered as being ejected into the condenser space continuously, and the liquid can be considered as flowing continuously back from the condenser into the evaporator. Under this condition, the vapor–liquid interchange in the network heat pipe is in a quasi-countercurrent mode. As a result, the network heat pipe can work very smoothly with a very small temperature fluctuation due to the pressure fluctuation in the heat pipe. Unlike the pulsating heat pipe, the vapor–liquid interchange in the network heat pipe is largely irregular and random around the periphery of the evaporator. The purpose of the network grooves in the present design is to provide a large number of paths for the vapor–liquid interchange and consequently to reduce the time period of the interchange cycle.

3. Experimental setup and procedure

The experimental setup, as shown schematically in Fig. 4(c), features a 360° rotation capability for the testing of the network heat pipe at different tilt angles, and includes a variable transformer, a cooling fan, and a scanning thermocouple thermometer connected to a computer and a chart recorder. A flexible electrical heater, which has a 0.0127-mm-thick etched foil encapsulated between two layers of 0.05 mm Kapton insulation, was chosen as the concentrated heat source. The dimensions of the heater are 9.86×37.5 mm^2. The heater was tightly pressed onto the bottom center of flat-plate network heat pipe by a specially designed clamp tool. The other side of the heater exposed to the surrounding air was well insulated, with negligible heat loss to the surrounding air. For various test surfaces, either nine or twelve thermocouples were used to measure the surface temperature distribution. One thermocouple was located very close to the heater, and the rest were dis-

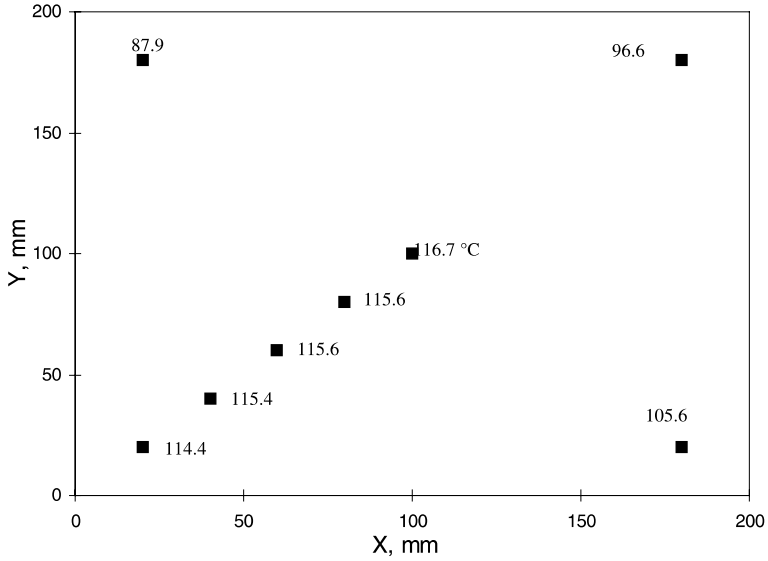

Fig. 5. Temperature distribution for HP1 on the top surface in a horizontal position (water charging ratio $\varphi = 0.64$, $q = 71.8$ W/cm^2, $T_h = 123.5$ °C.

tributed evenly on the top surface. Temperature data were taken by the scanning thermocouple thermometer that has ±0.4 °C accuracy and then sent to the computer through the serial port. The heat generated from the heater was spread by the network heat pipe and dissipated into the ambient air though natural and forced convection using a cooling fan. A chart recorder was used to record the possible temperature fluctuation near the heater. The overall uncertainty of the recorder from all sources is less than 0.5%. The experiment was carried out with water and methanol as the working fluids under different fill ratios, working temperature levels, inclination angles, and power inputs to the network heat pipes.

4. Experimental results

Figs. 5–7 show some typical temperature distributions on the top surface of the spreader for different heat fluxes from the heater that was located at the center of the network heat pipe. The heat pipe is in a horizontal orientation (Fig. 5) and uses water as the working fluid. The fluid-charging ratios were kept almost at a constant for all of the cases presented. The fluid-charging ratio is defined as the volume ratio of the liquid to the vapor space. The temperature distributions were rather uniform over most of the surface except for some corner regions along the periphery of the heat pipe. The value of T_h indicated in Fig. 5 was the temperature reading of the thermocouple at the heater on the bottom surface of the heat pipe. As mentioned in Section 1, the circulation of the working fluid is essential in order to facilitate heat transfer in the heat pipe. In order for the working fluid to travel from the center to the periphery, a relatively large amount of pressure drop is required to overcome the associated flow resistance. As a result of the two-phase saturated condition, a certain amount of temperature drop is created corresponding to this pressure drop. In addition, the flow of the working fluid in the corner is subject to the restrictions of the corner walls. Therefore, some stagnation flow regions may exist around the corners, and the temperatures around these regions are substantially lower due to the poor communication of the working fluid between the center and corner. It should be pointed out, however, that the performance of a network heat pipe is largely determined by the area-averaged temperature over the total heat dissipation surface. Although the temperature around the corner may be substantially lower, the surface area associated with the corner is relatively small. Therefore, the overall performance of the network heat pipe should not be significantly affected. The maximum heat flux achieved for the case presented in Fig. 5 was about 72 W/cm^2. The total heat input to the network heat pipe from the heater that corresponds to this maximum heat flux was 265 W. It should be noted that the maximum heat flux was limited by the capacity of the heater and not by the operating limits of the heat pipe.

Figs. 6 and 7 present testing results for the network heat pipes at tilt angles of 30° and 90°, respectively. For both orientations, the surface $X = 0$ was the bottom surface with reference to the gravitational field. As can be seen from the figures, the tilt angles have some adverse effects on the temperature distribution over the plate. The temperature distribution in the lower part of the plate is less uniform compared to the temperature distribution in the upper part of the plate. Because the charging ratios for both cases were more than 60%, the static liquid level should be above the heater at the

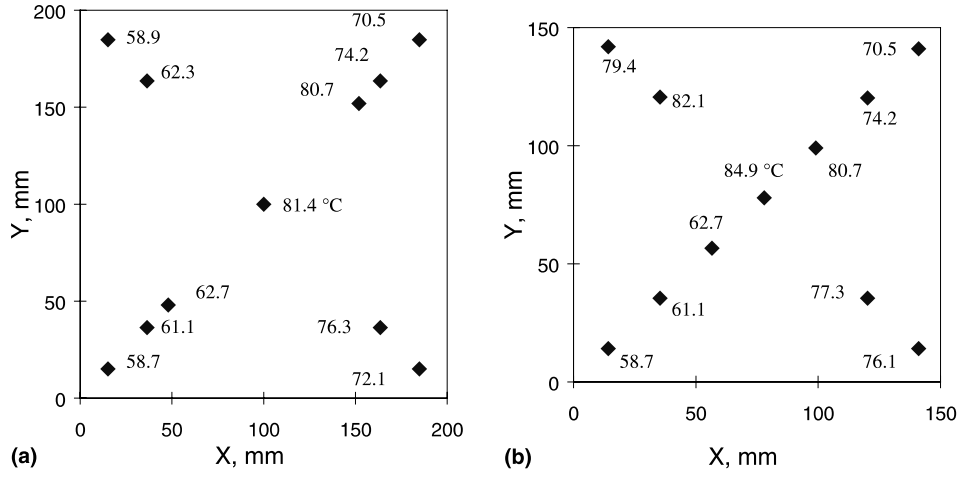

Fig. 6. Temperature distribution on the top surface with a tilt angle of 30° (water charging ratio $\varphi \approx 0.60$): (a) HP1, $q = 24.83$ W/cm^2, $T_h = 88.2$ °C; (b) HP2, $q = 25.39$ W/cm^2, $T_h = 83.2$ °C.

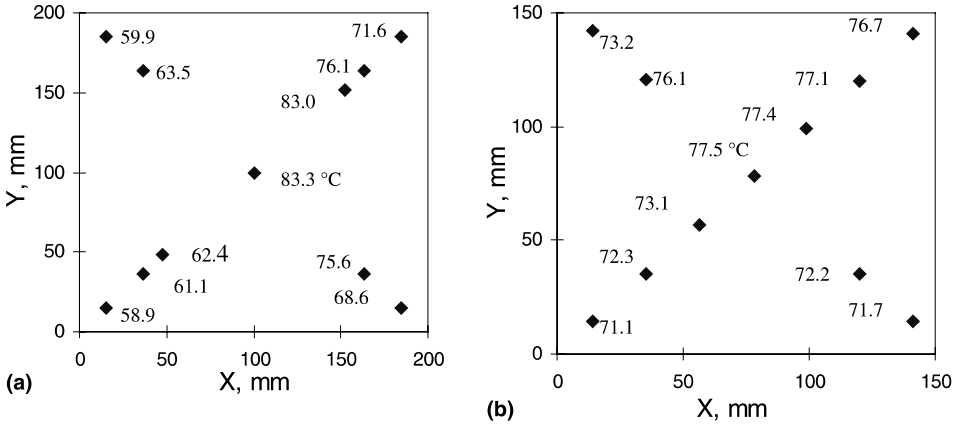

Fig. 7. Temperature distribution on the top surface in a vertical position (water charging ratio $\varphi \approx 0.60$): (a) HP1, $q = 29.24$ W/cm^2, $T_h = 89.7$ °C; (b) HP2, $q = 31.52$ W/cm^2, $T_h = 82.3$ °C.

center. Because of this, the access of liquid to the heated surface may not be a serious problem before the heat transfer limit is reached. The temperature discrepancy between the lower and upper portions of the heat pipe may be attributable to vigorous bubbles ascending under the buoyancy effect. Because less vapor bubbles were ejected into the lower half of the heat pipe, the fluid circulation in that region was significantly reduced.

To evaluate the overall performance of the network heat pipe, the thermal resistance of the heat pipe is compared with that of the empty sample that has the same size as the network heat pipe and a zero fluid-charging. Because of the zero fluid-charging, the heat transfer in the empty sample is solely due to conduction in the metal. The thermal resistances for both network heat pipes and empty samples are defined based on the following equation:

$$R_t = \frac{T_h - T_{s,ave}}{Q_{in}},$$

where T_h is the temperature of the heated surface. In the present study, it is the temperature reading of the thermocouple adjacent to the heater. $T_{s,ave}$ is the area-averaged temperature of the heat dissipation surface, and Q_{in} is the total heat input from the heater to the network heat pipe or the empty sample. Figs. 8 and 9 present the comparison of the thermal resistances between the network heat pipe HP1 and the empty sample for water and methanol as the working fluids, respectively. The thermal resistance for the heat pipe with water as the working fluid is 15–30 times smaller than that of the empty sample. Although the comparison for methanol is less favorable, the reduction of the thermal resistance is still on the order of 10. It should be pointed out that the comparison is between the heat pipe and the empty sample not between the heat pipe and the solid metal. In addition, the heat pipe in this study can spread a heat flux of over 100 W/cm^2, but the empty sample can only handle a heat flux less than 20 W/cm^2 at the same

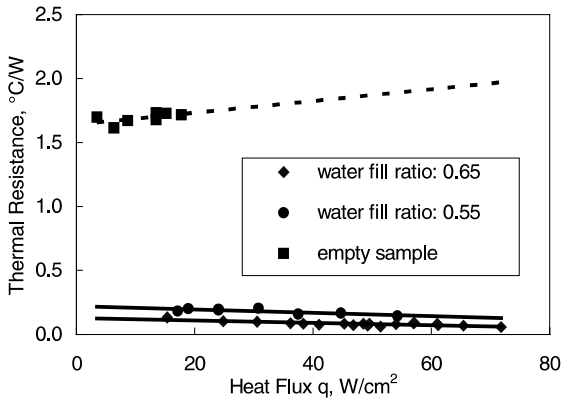

Fig. 8. Comparison of thermal resistances between network heat HP1 and its empty sample.

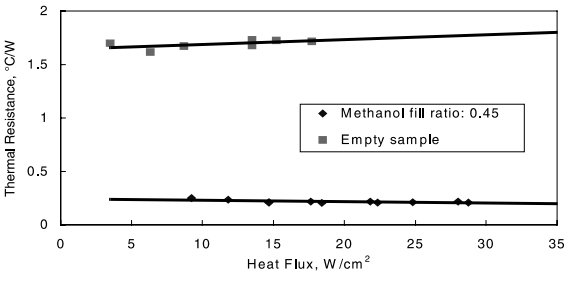

Fig. 9. Comparison of thermal resistances between HP1 and its empty sample.

highest temperature close to the heater. The influence of the fluid-charging ratio on the performance of the network heat pipe No. 1 and heat pipe No. 2 is shown in Fig. 10. For a given heat-pipe geometry, working fluid, and power input, it is believed that an optimal fluid-charge ratio would exist that provides the best performance under these given conditions. Another important factor for the spreader performance is the tilt angle. Fig. 11 presents some typical thermal resistances for HP1 at different tilt angles. The experimental results in Fig. 11 indicate that the network heat pipe functions best in a horizontal position without the influence of gravity and, therefore, is especially suited for aerospace applications. The thermal resistance is also a function of heat flux from the heater. At a higher heat flux, the thermal resistance was reduced to a substantially lower level compared to that at a lower heat flux.

Another criterion used to judge the performance of the network heat pipe is the magnitude of the temperature fluctuation. For this purpose, a chart recorder was utilized to monitor the change of temperature with time at different locations of the network heat pipe. Fig. 12 shows some representative temperature fluctuations of heat pipe No. 1 adjacent to the heater for different heat fluxes at the evaporator. The temperature fluctuation at the heated surface is believed to be due to the cyclic nucleate boiling at the evaporator. As the heat flux was increased, the amplitude of the fluctuation is seen to increase gradually. However, the temperature fluctuation was generally very small. Even for the case of $q = 61$ W/cm^2, the amplitude of the fluctuation was still only about 3 °C. Unlike the pulsating heat pipe, the temperature fluctuation of the network heat pipe was limited only to the heated surface. As shown in Fig. 13, the fluctuation was diminished for the temperature slightly away from the heater. The temperature fluctuation seems also to be influenced by the fluid-charging ratio. For a higher fluid-charging ratio, the amplitude of the fluctuation was substantially reduced (Fig. 14).

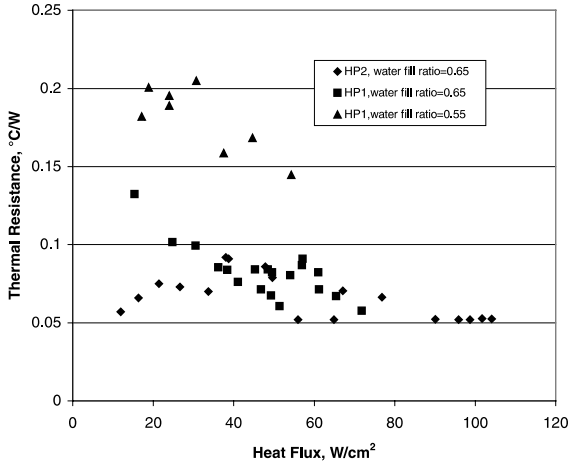

Fig. 10. Theremal resistance vs. heat flux at different charging ratios for HP1 and HP2.

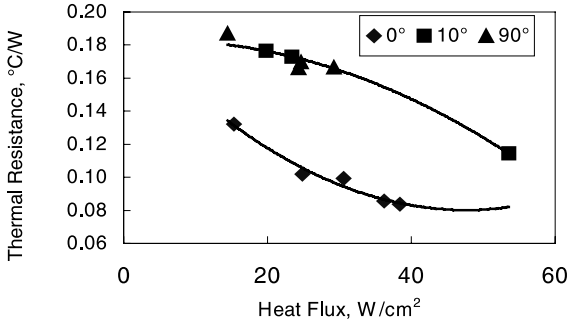

Fig. 11. Thermal resistance vs. heat flux at different inclination to horizontal plane.

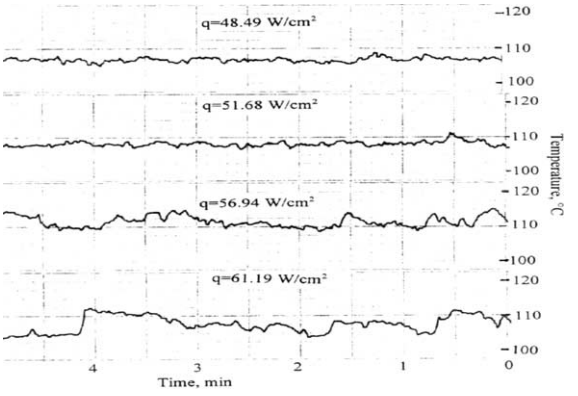

Fig. 12. Fluctuation of temperature close to heater center in a horizontal position (HP1, $\varphi = 65\%$).

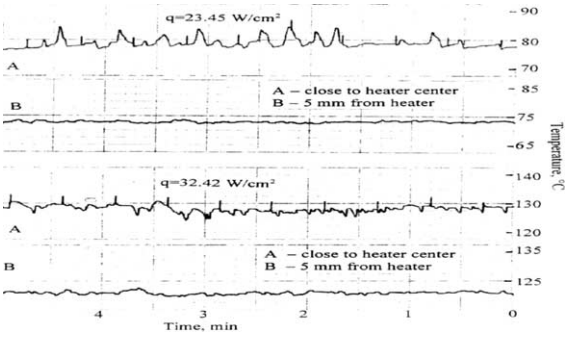

Fig. 13. Comparison of temperature fluctuations with an inclination of 10° (HP1, $\varphi = 61\%$).

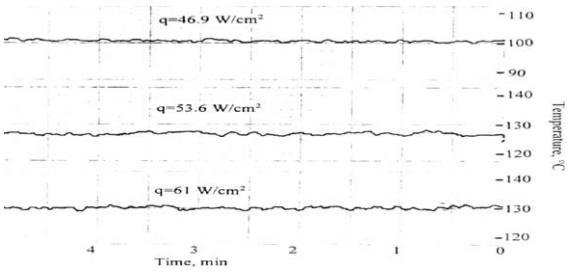

Fig. 14. Fluctuation of temperature close to heater center with inclination of 10° (HP1, $\varphi = 78\%$).

5. Conclusions and discussions

Based on the concept of the boiling heat transfer in a narrow space, two network heat pipes were fabricated and tested. The network heat pipe was a wickless heat pipe that is capable of spreading heat from a concentrated heat source to a large surface area with low manufacturing costs. The maximum heat flux achieved was more than 110 W/cm^2 with a total heat input of about 393 W. However, the heat pipe can achieve an even higher heat flux because the heat transfer capacity was limited by the electric heater in the present study, and not by the heat pipe itself. With regard to future research and development in this area, the following comments are in order:

1. The network heat pipe fabricated in this paper is only one of the possible network heat pipes. Based on the working mechanism of the network heat pipe discussed in this paper, network heat pipes with different configurations can be built to suit different specific applications. To enhance the heat dissipation, fins can be installed at the heat-dissipation surface for air-cooling purpose.
2. A porous wick structure may be provided at the interior surface of the network pipe for performance improvement, as shown in Fig. 15. Unlike for the wicked flat-plate heat pipe, the major function of the porous wick structure in the network heat pipe is not to provide the capillary pumping force for the return of the liquid condensate, but to retain the liquid during the cyclic boiling process and to enhance the boiling heat transfer at the heated surface. This may be especially important for a network heat pipe subject to a transient inertia force in an aerospace application.
3. The aforementioned network heat pipes feature crossed grooves that run throughout the entire plate. In order to reduce the flow resistance from the heated surface to the periphery of the plate, the crossed grooves may be eliminated in the condenser section. However, some crossed grooves are still retained in the evaporator section for the heat transfer enhancement. Finally, the network heat pipe may be simply formed by two plates with a narrow gap between them. On the heated surface, however, a layer of porous medium may be provided to provide nucleation sites for boiling at the heated surface. The porous medium can be sintered powders, screen wicks, machined grooves with reentrant cavities, or simply groove wick structures appearing in many conventional heat pipes.
4. Although the working mechanism of the network heat pipe has been described in detail in this paper, analytical modeling of the heat transfer process in the network heat pipe is needed. This work should provide some analytical or semi-empirical relations that can be used for the heat-pipe design. Optimization of the network heat-pipe structure is also important to increase the heat-transfer capacity of the heat pipe.

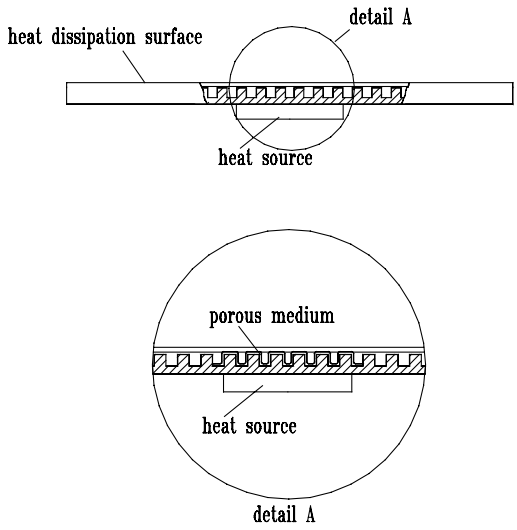

Fig. 15. Network heat pipe with porous wick in the evaporator section.

References

[1] A. Faghri, Heat Pipe Science and Technology, Taylor & Francis, London, 1995.
[2] Y. Cao, M. Gao, J.E. Beam, B. Donovan, Experiments and analyses of flat miniature heat pipes, ICCEC Paper No. 96456, 1996.
[3] H. Akachi, S. Motoya, S. Maezawa, Thermal performance of capillary tunnel type flat plate heat pipe, in: 7th International Heat Pipe Conference, Albuquerque, New Mexico, 1995.
[4] H. Akachi, F. Polasek, Pulsating heat pipe – review of the present state of the art, Technical Report ITRI ERL, 1995.
[5] S. Maezawa, A. Minamisawa, H. Akachi, Thermal performance of capillary tube thermosyphon, in: 7th International Heat Pipe Conference, Albuquerque, New Mexico, 1995.

[6] Y. Chang, S.C. Yao, Critical heat flux of narrow vertical annuli with closed bottoms, ASME J. Heat Transfer 105 (1983) 192–195.
[7] M.D. Xin, Y. Cao, Analysis and experiment of boiling heat transfer on T-shaped finned surfaces, Chem. Eng. Commun. 50 (1–6) (1987) 185–201.
[8] G.B. Wallis, One-dimensional Two Phase Flow, McGraw-Hill, New York, 1969.
[9] Y. Katto, S. Yokoya, K. Teraoka, Nucleate and transition boiling in a narrow space between two horizontal, parallel disk-surfaces, Bull. JSME 20 (143) (1977) 638–643.
[10] Y. Cao, M. Gao, High heat-flux network heat pipes employing boiling mechanisms in a narrow space, in: AIAA 32nd Thermophysics Conference, June 23, Atlanta, GA, 1997.